ISSN 0026-8933, Molecular Biology, 2010, Vol. 44, No. 6, pp. 939–947. © Pleiades Publishing, Inc., 2010.
Original Russian Text © T.S. Nepomnyashchikh, D.V. Antonets, L.R. Lebedev, I.P. Gileva, S.N. Shchelkunov, 2010, published in Molekulyarnaya Biologiya, 2010, Vol. 44, No. 6, pp. 1054–1063.

STRUCTURAL–FUNCTIONAL ANALYSIS OF BIOPOLYMERS AND THEIR COMPLEXES

UDC 571.27:577.322:578.23

3D Structure Modeling of Complexes Formed by CrmB TNF-Binding Proteins of Variola and Cowpox Viruses with Murine and Human TNFs

T. S. Nepomnyashchikh, D. V. Antonets, L. R. Lebedev, I. P. Gileva, and S. N. Shchelkunov

Vector State Research Center of Virology and Biotechnology, Federal Service for Surveillance in Consumer Rights Protection and Human Well-Being, Koltsovo, Novosibirsk region, 630559 Russia; e-mail: antonec@ngs.ru

Received March 16, 2010
Accepted for publication March 26, 2010

Abstract—Orthopoxviral genomes bear genes for a series of homologous secreted proteins binding tumor necrosis factor (TNF). Orthopoxvirus species have different sets of these proteins. Variola virus has only one protein of this series, CrmB. Although CrmB protein sequences are similar to each other, their physicochemical and biological properties show certain species-specific features. We constructed 3D models of complexes formed by TNF-binding domains of variola and cowpox viruses with murine and human TNFs. We also constructed corresponding models with a mutant human TNF. In this mutant TNF, the arginine residue at position 31 involved in receptor binding was replaced by glutamine, characteristic of murine TNF. Analysis of the models showed that the least stable complex should be that formed by cowpox virus CrmB with human TNF, and the Arg31/Gln substitution should significantly stabilize the interaction between cowpox CrmB and mutant human TNF. Experimental comparison of the abilities of recombinant variola and cowpox CrmB proteins to inhibit the cytotoxic action of TNFs confirmed the predictions.

DOI: 10.1134/S0026893310060117

Keywords: TNF, TNF-binding CrmB protein, molecular modeling, variola virus, cowpox virus

Proteins belonging to the families of TNF ligands and receptors are key regulators of cell development, proliferation, viability, and differentiation. They also orchestrate innate and antigen-specific responses of the immune system [1, 2]. At present, over 40 members of the TNF receptor family are known [2]. Most of them are transmembrane proteins of type I, whose extracellular fragments interact with ligands of the TNF family and intracellular domains support signal transduction by interacting with appropriate adaptor proteins [1, 2]. Although the amino acid sequences of proteins belonging to TNF receptors show low degrees of similarity (20–34%) [3], their TNF-binding domains have similar 3D structures. A characteristic feature of these proteins is the presence of one to six cysteine-rich domains (CRDs), pseudo repeats of approximately 40 aa in length. Typically, a TNF receptor protein (TNFR) has three or four such domains. Examples are TNFR I and TNFR II. The CRD boundaries are determined by intramolecular disulfide bridges between conservative cysteine residues [2]. The complexes of TNFRs and their ligands are heterohexamers, where three receptor molecules are bound to the homotrimeric ligand molecule. Each receptor molecule is adjacent to two ligand molecules, being located in a groove between them, but does not interact with other receptor molecules in the complex. The amino acids involved in ligand binding belong mainly to loop 50, located in CRD2, and to loop 90, located in CRD3 [1, 4].

Homologs of cellular TNF receptors encoded by orthopoxviruses have been described. They are soluble TNF-binding proteins: CrmB, CrmC, CrmD, and CrmE. Large quantities of these proteins are secreted by infected cells [5–8]. Different orthopoxviruses have different sets of TNF-binding proteins [9]. Cowpox virus (CPXV) has the greatest number of such proteins. Variola virus (VARV), of the same family, has only CrmB. It has been shown that poxviral TNF-binding proteins are important virulence factors, because viruses lacking the corresponding genes are attenuated to a marked extent [10, 11].

Elevated TNF expression is one of the factors determining the development of severe chronic inflammatory and/or autoimmune diseases in humans: rheumatoid arthritis, Crohn's disease, psoriasis, psoriatic arthropathy, etc. Anti-TNF therapy is successfully used to treat these diseases [12–15]. Study of the molecular bases of the interaction between orthopoxviral TNF-binding proteins and their cellular

Abbreviations: CPXV, cowpox virus; CRD, cysteine-rich domain; Crm, cytokine response modifier; h, human, LT, lymphotoxin; mh, mutant human; mu, murine; TNF, tumor necrosis factor; TNFR I and TNFR II, cellular TNF receptors of types I and II; VACV, vaccinia virus; VARV, variola virus; OD, optical density.

ligands is essential for understanding their biologic action. It can provide grounds for the development of new anti-TNF pharmaceuticals on the basis of these viral proteins. The main source of knowledge of receptor–ligand interactions is the 3D structure of their complexes. As the structures of CrmB proteins and their complexes with TNFs are unknown, we can approach to the solution of the problem by constructing models of such structures on the basis of structures of other TNF receptor proteins and their complexes with ligands obtained by X-ray structural analysis [16–18].

Here, we present our predictions of the efficiency of binding of murine (mu) and human (h) TNFs and some mutant human TNF forms (mhTNFs) to VARV-CrmB and CPXV-CrmB proteins on the basis of models of quaternary structures of the corresponding receptor–ligand complexes. The results of experimental verification of these predictions by in vitro comparison of the inhibiting action of these TNF-binding proteins on the cytotoxic effects of various TNFs are also presented.

EXPERIMENTAL

Materials. Plates (96-well) were purchased from Orange Scientific (United States); Grace's medium, antibiotics, and L-glutamine were from Gibco/BRL; and fetal calf serum was from BIOLOT (St. Petersburg, Russia). DMEM medium was manufactured by Vector (Koltsovo, Russia). Recombinant hTNF (6×10^7 U/mg) was kindly provided by Yu.N. Kozlova (Institute of Chemical Biology and Fundamental Medicine, Novosibirsk, Russia). Murine TNF (3×10^7 U/mg) [19] and muteins mhTNF(R31Q) (2×10^7 U/mg) [20] and mhTNF(E127Q) (7×10^6 U/mg) were isolated from the corresponding producer strains as described in [21]. Recombinant plasmid DNA encoding the mhTNF(E127Q) mutein was kindly provided by L.N. Shingareva (Shemyakin and Ovchinnikov Institute of Bioorganic Chemistry, Moscow, Russia). VARV-CrmB and CPXV-CrmB proteins had been obtained in our previous studies [19].

Cells. Experiments were performed with L929 murine fibroblast line stored in the cell culture collection at Vector. The cells were grown in DMEM with 2 mM L-glutamine, 100 U/ml penicillin, and 100 μg/ml streptomycin at 5% CO_2 and 37°C.

In vitro assay of the biologic activity of CrmB proteins. The activity of CrmB proteins was determined from their ability to inhibit the cytotoxic action of TNF on L929 murine fibroblast cells as described in [19]. The results are expressed as percentage of surviving cells in comparison with control samples without cytokines. Each measurement was done in triplicate, and the mean survival rate was calculated as:

$$(OD_{TNF+CrmB} - OD_{TNF})/(OD_{cells} - OD_{TNF}) \times 100\%.$$

Optical density was measured with a Microplate Reader EL_X808 (BIO-TEK Instruments, Inc., United States) at the wavelength 550 nm.

Modeling of the structure of TNF receptor domains of VARV-CrmB and CPXV-CrmB proteins and their complexes with muTNF, hTNF, and mhTNF. The modeling with Modeller software was based on the structure of the CrmE TNF-binding protein of vaccinia virus (VACV) (PDB ID:*2UWI*) [22]. The models of ligand–receptor complexes of VARV CrmB and CPXV CrmB with hTNF, mhTNF, and muTNF were obtained by superposition of the receptor and ligand structures onto the structure of the complex formed by human TNFR I (p55) with the lymphotoxin homotrimer (LT) (PDB ID: *1TNR*). The structures of hTNF (PDB ID: *1TNF*) or muTNF (PDB ID: *2TNF*) were taken as ligands. The mhTNF structures possessing amino acid substitutions were obtained with NOC software [23] by means of introduction of corresponding mutations to the *1TNF* sequence followed by local energy minimization. The energy minimization of the models was performed with NOC with an AMBER 2003 force field [24] or with FoldX software [25].

Analysis of models of ligand–receptor complexes. The adequacy of the models was assessed with ProCheck software [26]. The difference between the relative accessibilities of amino acid residues in soluble VARV- and CPXV-CrmB proteins and in the same proteins associated with various ligands, as well as the areas of contact with ligands were determined with NOC. The complementarity of the surfaces of molecules involved in the interaction was determined with SC program [27] integrated into the CCP4 package [28]. Data on the contacting amino acid residues of the receptor and ligand molecules were obtained with Biopython software [29]. Amino acids were considered contacting if the distance between the members of any pair of heavy atoms was no more than 4.2 Å. Additional contacting residues were determined as those whose C_β atoms were no more than 8 Å apart. The stability of the complexes was assessed by using the amino acid contact potential matrix BETM990101 [30]. Additional prediction of the stability of ligand–receptor complexes was obtained with FoldX. All programs for automated analysis and data processing were written in Python (http://python.org).

RESULTS AND DISCUSSION

The construction of our models was based on the structure of the VACV-CrmE TNF-binding protein, which is the closest homolog of the CrmB proteins studied in our work [18]. The similarity between the amino acid sequences of the TNF receptor domains of the CrmE and orthopoxviral CrmB proteins is approximately 50%. The accession code of CrmE in PDB is *2UWI*. Like mammalian TNF receptors, the TNF-binding domain of orthopoxviral CrmB proteins consists of tandemly arranged CRDs, each containing two structural units with one or two disulfide bridges. The units are conventionally named A and B with regard to topology. With regard to the number of disulfide

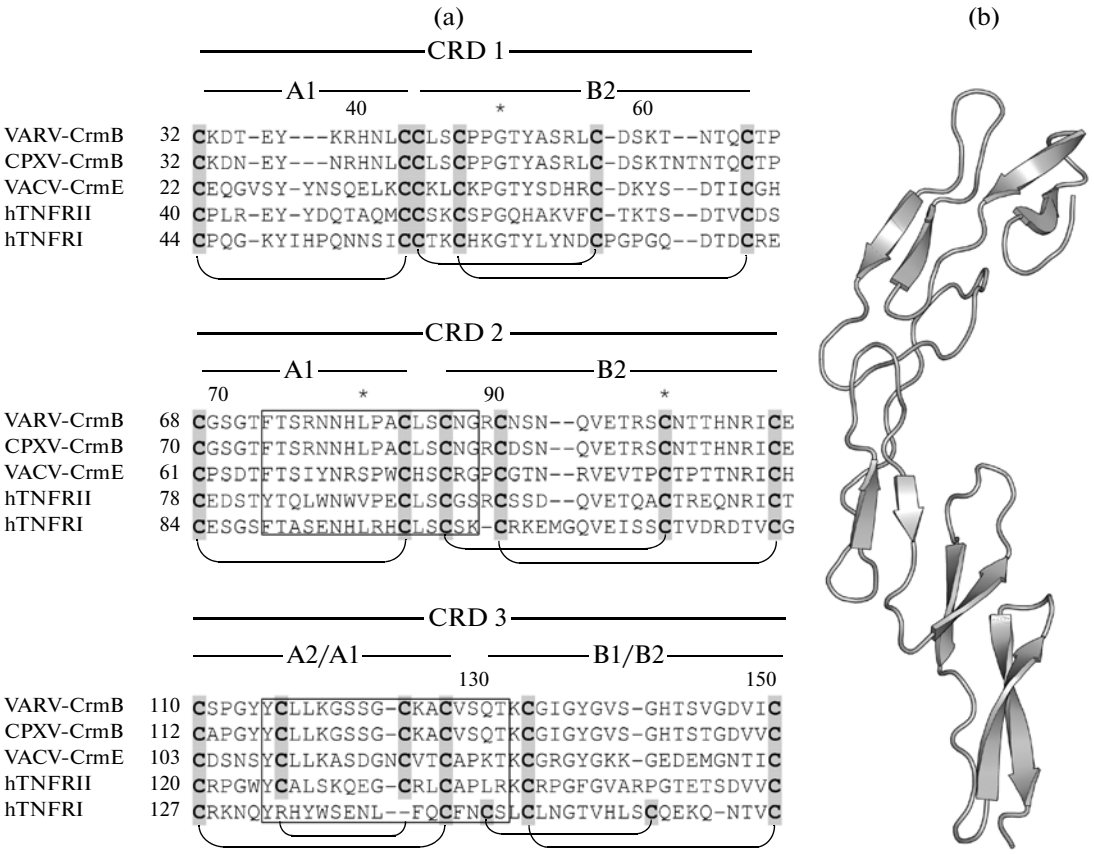

Fig. 1. Alignment of the TNF receptor domains of the VARV-CrmB and CPXV-CrmE proteins with human TNFR I and TNFR II and the 3D structure of the TNF receptor domain of VARV-CrmB. (a) Alignment of the sequences of cysteine-rich domains (CRD1-3). Units A1 and B1 form the CRD1 and CRD2 units of the proteins under consideration. The cysteine-rich domains of human CrmB, CrmE, and TNFR II are built of A2 and B2. In TNFR I, CRD3 contain A1 and B2. Boxes indicate binding sites: loops 50 and 90. Conservative cysteine residues are shown in boldface with gray filling. Brackets indicate disulfide bridges. (b) Band model of the 3D structure of the TNF receptor domain in VARV-CrmB (CRD1-3). Elements of the secondary structure are shown. The image was constructed with PyMOL [42]. Data reported in [18] are invoked.

bridges within the unit, they are named A1, A2 and B1, B2 [4, 18]. Alignment of the amino acid sequences of CRD1–CRD3 of the proteins VARV-CrmB, CPXV-CrmB, VACV-CrmE, and human TNFRs of types I and II shows that the CRD3 of the CrmB protein, as well as in CrmE and TNFR II, consists of A1–B2 units (Fig. 1a), unlike TNFR I, whose receptor domain includes A1–B2 (CRD1), A1–B2 (CRD2), and A2–B1 (CRD3). Thus, CrmE, like CrmB, is closer to TNFR II than to TNFR I, and it is the best prototype for the model of TNF-receptor domains of CrmB proteins.

We applied the Modeller program [22], commonly used for modeling 3D structures of proteins on the basis of their similarity, to the construction of models of TNF receptor domains of the CrmB proteins from VARV (Fig. 1b) and CPXV. Check of these models with ProCheck software confirmed their satisfactory adequacy [26]. The models of VARV-CrmB and CPXV-CrmB differ little. The root mean square deviation (RMSD) between the centers of their C_β atoms is approximately 0.98 Å. The mean RMSD value in the comparison of coordinates of all heavy atoms is 1.6 Å.

It appears that CrmB associated with TNF has a structure typical of complexes of TNF receptor proteins with their ligands: the homotrimeric upturned bell-shaped ligand (TNF) molecule interacts with three receptor (CrmB) molecules located in grooves between ligand subunits. Each CrmB molecule is linked to two TNF subunits but does not interact with other CrmB molecules. The models of ligand–receptor complexes were obtained by superposition of the structures of CrmB (VARV or CPXV) and the TNF homotrimer (hTNF or muTNF) onto the structure of the complex of TNFR I with the LT homotrimer (PDB ID: *1TNR*). The structures of hTNF (PDB ID: *1TNF*) or muTNF (PDB ID: *2TNF*) were taken as ligands. The following models were obtained: VARV-CrmB + hTNF, VARV-CrmB + muTNF, CPXV-CrmB + hTNF, and CPXV-CrmB + muTNF. The model of the 3D structure of VARV-CrmB + hTNF is shown in Fig. 2 as an example.

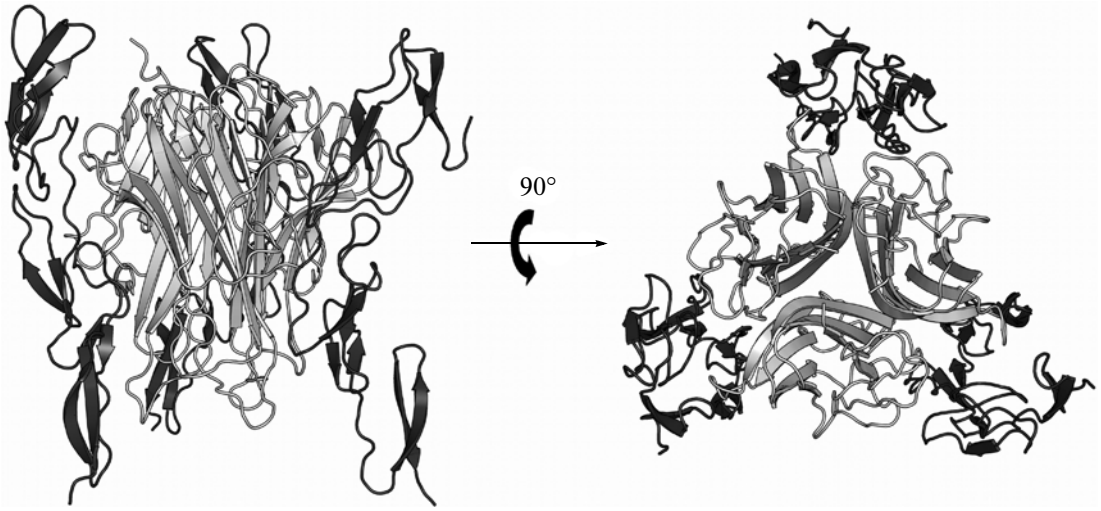

Fig. 2. The heterohexameric complex formed by the hTNF homotrimer bound to three VARV-CrmB molecules. Only TNF receptor domains are shown. The TNF homotrimer, shown in gray, has the shape of an upturned bell. Oblong CrmB molecules (dark-gray) are located in grooves between TNF subunits. Each receptor molecule is adjacent to two TNF molecules but does not interact with other receptor molecules. The band models shown in the figure illustrate secondary structure elements of TNF and TNF receptor domains of CrmB. The image was constructed with PyMOL [42].

To predict the stability of the ligand–receptor complexes CrmB + TNF, we extracted information on contacting amino acid residues of the receptor chain (single CrmB molecule) and the homotrimeric ligand from the models constructed with BioPDB [31]. Amino acid residues were considered contacting if the distance between members of at least one heavy atom pair did not exceed 4.2 Å [32]. We also determined contacting amino acids from the distance between their C_β atoms. For glycine residues, coordinates of their C_α atoms were considered. In this method, residues were considered contacting if their C_β atoms were no more than 8 Å apart [33]. The binding of the CrmB monomer to hTNF and muTNF homotrimers was assessed from the additive amino acid contact potential matrix BETM990101 [30]. The potentials were expressed in RT units, where R is the gas constant and T is thermodynamic temperature [30]. The potentials in stable complexes are negative: the lower is the potential value and the more stable is the complex. The prediction results are shown in Table 1. When contacting amino acids are determined as those in which members of at least one heavy atom pair are no more than 4.2 Å apart, the predicted contact potential

Table 1. Stability of the complexes of VARV-CrmB and CPXV-CrmB with muTNF, hTNF, and mhTNF(R31Q) predicted with the amino acid contact potential matrix BETM990101 [30]

Calculation of contact potentials						
A						
	CPXV-CrmB			VARV-CrmB		
Threshold distance, Å	hTNF	mhTNF(R31Q)	muTNF	hTNF	mhTNF(R31Q)	muTNF
4.2	–0.38	–0.50	–2.05	–0.99	–1.14	–1.99
B						
	CPXV-CrmB			VARV-CrmB		
Threshold distance, Å	hTNF	mhTNF(R31Q)	muTNF	hTNF	mhTNF(R31Q)	muTNF
8.0	–0.86	–1.01	–1.40	–1.27	–1.16	–3.65

Note: Values of the contact potentials of CrmB monomers with TNF homotrimers are expressed in RT units. Contact potentials were calculated by two methods: A—the contact between members of a pair of amino acids is defined as the threshold distance within 4.2 Å for at least one pair of heavy atoms; B—the distance between corresponding C_β atoms is no more than 8 Å.

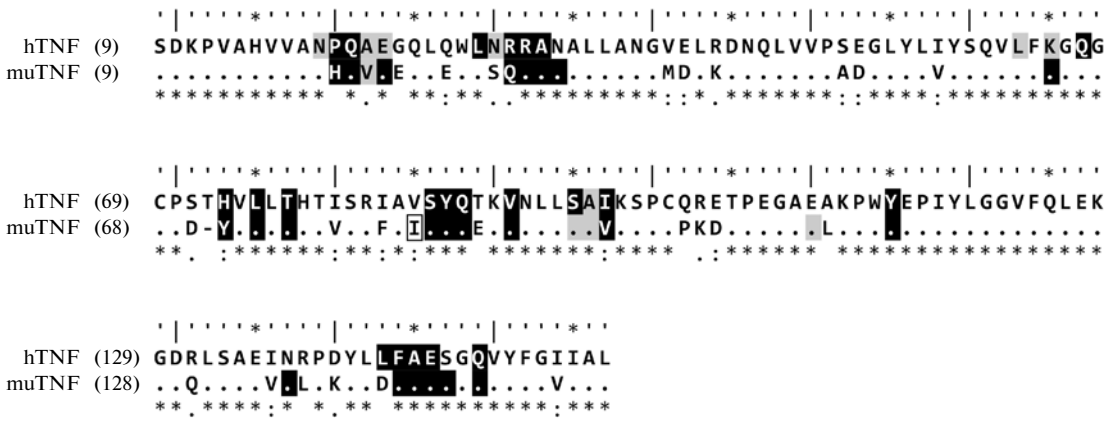

Fig. 3. Alignment of the hTNF and muTNF sequences. Colored letters indicate amino acid residues located no farther than 5 Å from residues of the CrmB receptor protein. White letters on black indicate residues located no farther than 5 Å from both VARV-CrmB and CPXV-CrmB, letters on gray indicate residues at distances no more than 5 Å from VARV-CrmB, and boxed letters indicate those from CPXV-CrmB. Symbols beneath the aligned sequences indicate: (*) identical amino acids, (:) conservative amino acid substitutions, and (.) semiconservative substitutions (BLOSUM62). The numbering corresponds to that accepted in the corresponding PDB entries: *1TNF* and *2TNF*.

between the CPXV-CrmB monomer with the hTNF homotrimer is −0.38 and that with the muTNF homotrimer is −2.05. The values of the contact potential of VARV-CrmB with the hTNF and muTNF homotrimers are −0.99 and −1.99, respectively. It follows from Table 1 that the interaction of CPXV-CrmB with muTNF is significantly more stable than with hTNF nearly in the whole range of threshold distances. The VARV-CrmB complex with muTNF is also predicted to be more stable than with hTNF. If we assume that contacting amino acids are those whose C_β atoms are no more than 8 Å apart, the contact potential of CPXV-CrmB with hTNF is −0.86 and that with muTNF is −1.4. The contact potentials of VARV-CrmB with hTNF and muTNF are −1.27 and −3.65, respectively (Table 1).

Additional predictions of the interaction energies of CPXV-CrmB with hTNF and muTNF were done with FoldX [25]. They also showed that the complex of CPXV-CrmB with the murine TNF homotrimer should be more stable than with the human homotrimer: −5.64 and −2.69 kcal/mol, respectively.

Analysis of the models of the ligand–receptor complexes and amino acid sequences of hTNF and muTNF revealed amino acids apparently involved in the binding of these cytokines to CrmB proteins (Fig. 3). Here are the differences between amino acids involved in binding to both VARV-CrmB and CPXV-CrmB: P20 in hTNF corresponds to H in muTNF, R31 corresponds to Q, H73 corresponds to Y, and I106 corresponds to V. We analyzed putative effects of the substitutions in the human TNF to the stability of the interaction of mutant human TNFs with VARV-CrmB and CPXV-CrmB. We also considered other substitutions adjacent to CrmB binding sites and, probably, also affecting the binding to CrmB proteins: A22V, G24E, N30S, I97V, S71D, T72D, T89E, R138L, and L143D.

Models of complexes formed by VARV-CrmB and CPXV-CrmB with mutant human TNFs possessing the listed amino acid substitutions were obtained by introduction of mutations into hTNF in corresponding ligand–receptor complexes simulated with FoldX. Then predictions of complex stability were done with FoldX. According to these predictions, the substitutions T89E, R31Q, H73Y, and G24E in hTNF are most favorable for binding to CPXV-CrmB, and P20H loosens this binding. Other mutations are predicted to insignificantly affect the stability of CPXV-CrmB complexes with corresponding mutant hTNFs (Table 2). The substitutions L143D, R31Q, and H73Y in hTNF are most favorable for interaction with VARV-CrmB, whereas P20H and I97V loosen the complexes (Table 2). For the mutant human TNF possessing the substitution R31Q, we also analyzed the stability of complexes with VARV-CrmB and CPXV-CrmB with the amino acid contact potential matrix BETM990101 as described above. The predicted contact potentials of CPXV-CrmB with the mhTNF(R31Q) homotrimer and hTNF are −0.5 and −0.38, respectively, provided that the distance between members of at least one pair of heavy atoms of contacting residues is no more than 4.2 Å (Table 1). The corresponding contact potentials predicted with the proviso that the distance between C_β atoms of residues regarded as contacting is no more than 8 Å are −1.01 and −0.86 (Table 1). The energies of interaction of CPXV-CrmB with the homotrimers mhTNF(R31Q) and hTNF predicted with FoldX are −3.69 and −2.69 kcal/mol, respectively (Table 2). The results of both approaches indicate that the R31Q mutation in human TNF should stabilize the complex with CPXV-CrmB. We also constructed models of complexes of VARV-CrmB and CPXV-CrmB with the mutant human TNF(E127Q) species. Analysis of these models with FoldX showed that this substitution

Table 2. Predicted energies of the interaction of VARV-CrmB and CPXV-CrmB monomers with the hTNF homotrimer and with mutant hTNF species

Mutant human TNF	**E**, kcal/mol	
	CPXV-Crmb	VARV-CrmB
WT	***−2.69***	***−1.67***
R31Q	***−3.69***	***−4.67***
P20H	−1.36	0.54
A22V	−2.89	−1.75
G24E	−3.41	−2.03
N30S	−2.73	−1.95
S71D	−2.57	−1.55
T72D	−2.63	−1.61
H73Y	−3.71	−2.93
T89E	−3.89	−2.05
I97V	−3.13	−0.85
E127Q	***−1.99***	***−1.37***
R138L	−2.70	−1.79
L143D	−2.29	−5.25

Note: Interaction energies were assessed with FoldX software [25]. Amino acid substitutions in the hTNF sequence are shown in column 1, *WT* indicating the wild-type hTNF sequence. Experimentally investigated TNF species are shown in boldface.

should reduce the interaction of mhTNF(E127Q) with CPXV-CrmB and, to a lesser extent, that with VARV-CrmB (Table 2).

The predicted contact potentials of CrmB with various TNFs, as well as interaction energies calculated with FoldX, are not accurate quantitative parameters of ligand–receptor affinity. They provide merely comparative characterization of models constructed and indicate whether particular amino acid substitutions in TNF are favorable or unfavorable for binding to CrmB.

As data from the literature confirm that single amino acid substitutions at positions 31–33 of TNF are significant for interaction with its receptor proteins [34–37], we tested the ability of VARV-CrmB and CPXV-CrmB to inhibit the cytotoxic action of mhTNF(R31Q) in experiments. We also performed experiments with mhTNF(E127Q).

Inhibition of the cytotoxic effect of hTNF, muTNF, and mhTNF(R31Q) by CPXV-CrmB and VARV-CrmB was quantitatively assayed in L929 murine fibroblasts. It was found that VARV-CrmB equally efficiently inhibited the cytotoxic effects of muTNF, hTNF, mhTNF(R31Q) and mhTNF(E127Q) (Fig. 4). CPXV-CrmB inhibited the activity of muTNF and mhTNF(R31Q) almost equally efficiently, but showed much lower inhibiting activity against hTNF and virtually no activity against mhTNF(E127Q) (Fig. 4b). Thus, the experiment confirmed the prediction of the stabilizing effect of the R31Q substitution in hTNF on the complex with CPXV-CrmB and the negative effect of E127Q on the stability of the complex with CPXV-CrmB. Although we predicted that the VARV-CrmB + muTNF complex should be more stable than VARV-CrmB + hTNF (in agreement with the reported data that the K_d values of these complexes were 20×10^{-12} M and 22.3×10^{-11} M, respectively [38]), our experiments showed no difference in the biologic activity of VARV-CrmB against muTNF, hTNF, or mhTNF(R31Q). The comparison of the biologic activities of CPXV-CrmB and VARV-CrmB against hTNF, muTNF, and mhTNF indirectly reflects the stabilities of the corresponding ligand–receptor complexes but cannot be a quantitative index of the affinity of the receptor proteins towards the ligands.

Studies of TNFR I and CrmE have shown that the modeling of complexes of TNF receptor proteins with their ligands is hampered by the significant mobility of CRD2 with respect to CRD3 in TNF receptor proteins [17, 18]. Moreover, the ligands have slight structural differences between the soluble and receptor-bound states [39]. The hypothesis of structural changes in the receptors and/or ligands is supported by analysis of complementarity of molecular surfaces between TNF-binding proteins and their homotrimeric ligands reported in [18]. The values of complementarity of Sc surfaces of the TNFR I complex with lymphotoxin and of the complex of death receptor 5 (DR5) with its ligand (TRAIL–TNF-like apoptosis-inducing ligand) are 0.64 and 0.62, respectively. For the model of the CrmE + hTNF complex constructed in the same study, this value is –0.45. Therefore, Graham et al. [18] conclude that the 3D structure of the CrmE + TNF complex could not be adequately predicted by modeling based on similarity.

Apparently, the complementarity between the receptor and ligand surfaces cannot be a reliable criterion for assessment of model adequacy in this case. We suggested a greater complementarity of TNRF I surfaces to the ligands than in the case of TNRF II. It is known that TNFR I (p55) is more affine to TNF than TNFR II (p75): the K_d values of p55 and p75 complexes with human TNF are 1.9×10^{-11} M and 4.2×10^{-10} M, respectively. As opposed to TNFR II, TNFR I forms stable complexes with soluble TNF [40]. We simulated complexes of various TNFs with CPXV-CrmB and VARV-CrmB where the structure of p55 (1TNR) was used as a prototype for TNF-binding proteins. The complementarity values for the molecule surfaces of CPXV-$CrmB_{1TNR}$ and VARV-$CrmB_{1TNR}$ with regard to muTNF and hTNF were 0.526, 0.615 and 0.472, 0.478, respectively. The contact areas for these models were 1122, 1045 and 993, 960 Å^2, respectively. The predicted values of the contact potential of the CPXV-$CrmB_{1TNR}$ monomer with the muTNF and hTNF homotrimers in the case of a contact of at least one pair of heavy atoms at a distance

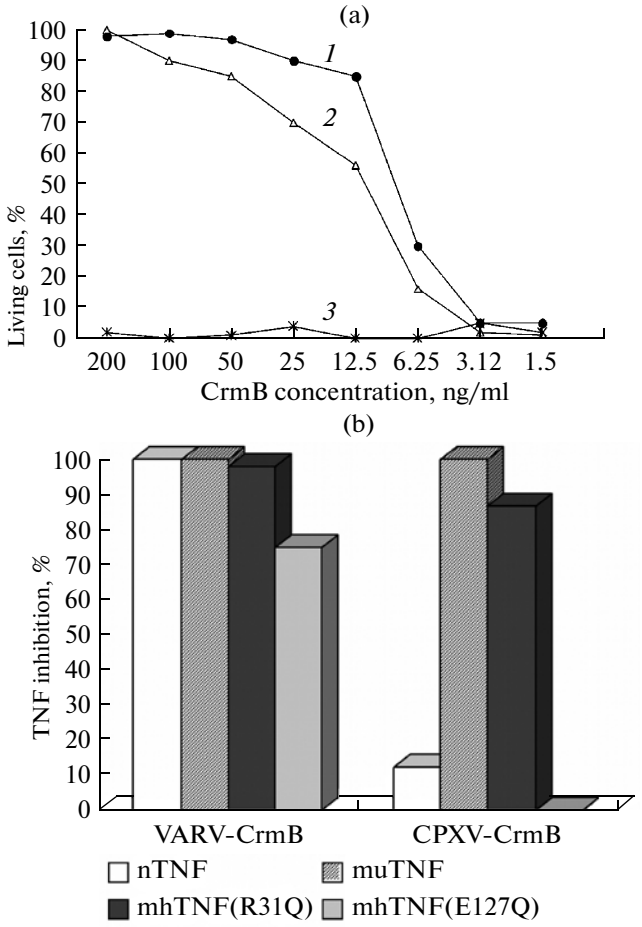

Fig. 4. In vitro inhibition of the cytotoxic action of TNF by CrmB proteins. (a) inhibition of mhTNF(R31Q) in L929 cells by viral TNF-binding proteins. X-Axis: TNF concentrations in plate wells. *1*—L929 + mhTNF(R31Q) + VARV-CrmB; *2*—L929 + mhTNF(R31Q) + CPXV-CrmB; *3*—L929 + mhTNF(R31Q). (b) the concentration of VARV-CrmB providing 50% protection from a sixfold 50% cytotoxic hTNF dose in L929 cells is taken to be 100%. Other values are calculated as $([\text{VARV-CrmB}]_{50\%}/[\text{CrmB}]_{50\%}) \times 100\%$.

within 4.2 Å were –0.12 and –1.49, respectively. Corresponding values for complexes of VARV-CrmB_{1TNR} with mu- and hTNF were 1.49 and –0.43. Thus, the CPXV-CrmB complex with hTNF should be much more stable than with muTNF, and the complex VARV-CrmB + muTNF should be unstable. With determination of amino acids as contacting if the distance between their C_β atoms is no more than (≤8 Å), all complexes were predicted to be unstable. The contact potential values of CPXV-CrmB with muTNF and hTNF and of VARV-CrmB with muTNF and hTNF were 2.25, 2.29 and 1.47, 2.69, respectively. This prediction disagrees with the experimental biologic activities of VARV-CrmB and CPXV-CrmB against muTNF and hTNF (Fig. 4).

In models of complexes with CPXV-CrmB and VARV-CrmB with CrmE (*2UWI*) as a prototype, the complementarity values for the receptor molecule surfaces with regard to muTNF and hTNF were 0.441, 0.465 and 0.431, 0.542. The corresponding contact areas were 901, 849 and 950, 933 Å^2. It is expected from the predicted contact potentials that the complex of CPXV-CrmB with muTNF should be more stable than with hTNF (Table 1). This conclusion is confirmed by prediction of the interaction energies between CrmB proteins and their ligands with FoldX (Table 2). It is also in agreement with the results of in vitro experiments on inhibition of the cytotoxic action of mu- and hTNF by CrmB proteins (Fig. 4).

Thus, the CPXV-CrmB models constructed on the basis of the structure of hTNERI show greater complementarity of the contact surface with ligands than corresponding models constructed from CrmE as a prototype. However, the stability of ligand–receptor complexes constructed on the basis of p55 disagrees with experimental results. In contrast, predictions for models based on CrmE agree with the biologic properties of VARV-CrmB and CPXV-CrmB experimentally investigated here and in other studies [38, 41].

CONCLUSIONS

It is reasonable to suggest that the smaller complementarity of the surface to the ligand is a characteristic feature of type II TNF receptors. The CrmE protein (*2UWI*) is presently the only item of this sort in the spatial structure bank (PDB). Probably, the earlier conclusion that the complexes of TNF receptor proteins with TNF cannot be applied to structure modeling was peremptory. It was made on the basis of the significant mobility of the structures of TNF receptor proteins and low complementarity of the surfaces of ligand–receptor complexes. This problem can be decisively solved by experimental analysis of the 3D structures of complexes between type II TNF receptors and their ligands.

The in vitro biologic activities of VARV-CrmB and CPXV-CrmB with regard to murine and human TNFs and to two mutant human TNFs agree with the inferences from 3D models of the corresponding ligand–receptor complexes. In our opinion, the models can be useful for understanding the molecular machinery supporting the interaction between orthopoxviral TNF receptor proteins and their ligands, design of mutant VARV-CrmB species more efficiently binding human TNF, and development of new pharmaceuticals for anti-TNF therapy on the basis of viral TNF-binding proteins.

ACKNOWLEDGMENTS

This work was supported by the Russian Foundation for Basic Research, project 09-04-00055.

REFERENCES

1. Locksley R.M., Killeen N., Lenardo M.J. 2001. The TNF and TNF receptor superfamilies: Integrating mammalian biology. *Cell*. **104**, 487–501.
2. Hehlgans T., Pfeffer K. 2005. The intriguing biology of the tumour necrosis factor/tumour necrosis factor receptor superfamily: Players, rules and the games. *Immunology*. **115**, 1–20.
3. Borysenko C.W., Furey W.F., Blair H. C. 2005. Comparative modeling of TNFRSF25 (DR3) predicts receptor destabilization by a mutation linked to rheumatoid arthritis. *Biochem. Biophys. Res. Commun*. **328**, 794–799.
4. Naismith J.H., Sprang S.R. 1998. Modularity in the TNF-receptor family. *Trends Biochem. Sci*. **23**, 74–79.
5. Hu F.Q., Smith C.A., Pickup D.J. 1994. Cowpox virus contains two copies of an early gene encoding a soluble secreted form of the type II TNF receptor. *Virology*. **204**, 343–356.
6. Smith C.A., Hu F.Q., Smith T.D., Richards C.L., Smolak P., Goodwin R.G., Pickup D.J. 1996. Cowpox virus genome encodes a second soluble homologue of cellular TNF receptors, distinct from CrmB, that binds TNF but not LT alpha. *Virology*. **223**, 132–147.
7. Loparev V.N., Parsons J.M., Knight J.C., Panus J.F., Ray C.A., Buller R.M., Pickup D.J., Esposito J.J. 1998. A third distinct tumor necrosis factor receptor of orthopoxviruses. *Proc. Natl. Acad. Sci. USA*. **95**, 3786–3791.
8. Saraiva M., Alcami A. 2001. CrmE, a novel soluble tumor necrosis factor receptor encoded by poxviruses. *J. Virol*. **75**, 226–233.
9. Cunnion K.M. 1999. Tumor necrosis factor receptors encoded by poxviruses. *Mol. Genet. Metab*. **67**, 278-282.
10. Upton C., Macen J.L., Schreiber M., McFadden G. 1991. Myxoma virus expresses a secreted protein with homology to the tumor necrosis factor receptor gene family that contributes to viral virulence. *Virology*. **184**, 370–382.
11. Reading P.C., Khanna A., Smith G.L. 2002. Vaccinia virus CrmE encodes a soluble and cell surface tumor necrosis factor receptor that contributes to virus virulence. *Virology*. **292**, 285–298.
12. Feldmann M., Maini R.N. 2001. Anti-TNF alpha therapy of rheumatoid arthritis: What have we learned? *Annu. Rev. Immunol*. **19**, 163–196.
13. Brandt J., Braun J. 2006. Anti-TNF-alpha agents in the treatment of psoriatic arthritis. *Expert Opin. Biol. Ther*. **6**, 99–107.
14. Palladino M.A., Bahjat F.R., Theodorakis E.A., Moldawer L.L. 2003. Anti-TNF-alpha therapies: The next generation. *Nature Rev. Drug. Discov*. **2**, 736–746.
15. Nepomnyashchikh T.S., Antonets D.V., Gileva I.P., Shchelkunov S.N. 2007. Diseases caused by disturbances in TNF and IFNγ production and modern approaches to their treatment. *Usp. Sovrem. Biol*. **127**, 576–587.
16. Banner D.W., D'Arcy A., Janes W., Gentz R., Schoenfeld H.J., Broger C., Loetscher H., Lesslauer W. 1993. Crystal structure of the soluble human 55 kd TNF receptor-human TNF beta complex: Implications for TNF receptor activation. *Cell*. **73**, 431–445.
17. Naismith J.H., Devine T.Q., Kohno T., Sprang S.R. 1996. Structures of the extracellular domain of the type I tumor necrosis factor receptor. *Structure*. **154**, 1251–1262.
18. Graham S.C., Bahar M.W., Abrescia N.G., Smith G.L., Stuart D.I., Grimes J.M. 2007. Structure of CrmE, a virus-encoded tumour necrosis factor receptor. *J. Mol. Biol*. **372**, 660–671.
19. Gileva I.P., Ryazankin I.A., Nepomnyashchikh T.S., et al. 2005. Expression of genes for orthopoxviral TNF-binding proteins in insect cells and investigation of the recombinant TNF-binding proteins. *Mol. Biol*. (Moscow) **39**, 218–225.
20. Sandakhchiev L.S., Merzlikin N.V., Pustoshilova N.M., Istomina N.N., Lebedev L.R., Svyatchenko M.I., Danilenko E.D., Masycheva V.I., Usova S.V. 1998. Some biological properties of human tumor necrosis factor alpha. *Onkologiya*. **125**, 89–92.
21. Pustoshilova N.M., Kileva E.V., Denisova L.Ya., Shingareva N.V., Masycheva V.I., Korobko V.G., Denisov L.A., Sandakhchiev L.S., Kalinin Yu.T. 1994. RF Patent no. 1438240.
22. Eswar N., Marti-Renom M.A., Webb B., Madhusudhan M.S., Eramian D., Shen M., Pieper U., Sali A. 2006. Comparative protein structure modeling with MODELLER. *Current Protocols in Bioinformatics*. 15, 5.6.1–5.6.30. URL http://salilab.org/modeller.

23. Chen M.E., Cang H.X., Nymeyer H. 2007. NOC: Free molecular explorer for protein structure visualization, validation and analysis. NOC 3.01. URL http://noch.sourceforge.net.

24. Duan Y., Wu C., Chowdhury S., Lee M.C., Xiong G., Zhang W., Yang R., Cieplak P., Luo R., Lee T., Caldwell J., Wang J., Kollman P. 2003. A point-charge force field for molecular mechanics simulations of proteins based on condensed-phase quantum mechanical calculations. *J. Comput. Chem*. **24**, 1999–2012.

25. Schymkowitz J., Borg J., Stricher F., Nys R., Rousseau F., Serrano L. 2005. The FoldX web server: An online force field. *Nucleic Acids Res*. **33**, 382–388.

26. Laskowski R.A., MacArthur M.W., Moss D.S., Thornton J.M. 1993. PROCHECK: A program to check the stereochemical quality of protein structures. *J. Appl. Cryst*. **26**, 283–291.

27. Lawrence M.C., Colman P.M. 1993. Shape complementarity at protein/protein interfaces. *J. Mol. Biol*. **234**, 946–950.

28. Collaborative Computational Project, Number 4. 1994. "The CCP4 Suite: Programs for Protein Crystallography". *Acta Cryst*. **D50**, 760–763. URL http://www.ccp4.ac.uk/

29. Chapman B.A., Chang J.T. 2000. Biopython: Python tools for computational biology. *ACM SIGBIO Newsletter*. **20**, 15–19. URL http://www.biopython.org.

30. Betancourt M.R., Thirumalai D. 1999. Pair potentials for protein folding: Choice of reference states and sensitivity of predicted native states to variations in the interaction schemes. *Protein Sci*. **8**, 361–369.

31. Hamelryck T., Manderick B. 2003. PDB file parser and structure class implemented in Python. *Bioinformatics*. **19**, 2308–2310.

32. Khare S.D., Dokholyan N.V. 2006. Common dynamical signatures of familial amyotrophic lateral sclerosis-associated structurally diverse Cu, Zn superoxide dismutase mutants. *Proc. Natl. Acad. Sci. USA*. **103**, 3147–3152.

33. Grana O., Baker D., MacCallum R.M., Meiler J., Punta M., Rost B., Tress M.L., Valencia A. 2005. CASP6 assessment of contact prediction. *Proteins*. **61**, 214–224.

34. Loetscher H., Stueber D., Banner D., Mackay F., Lesslauer W. 1993. Human tumor necrosis factor alpha (TNF alpha) mutants with exclusive specificity for the 55-kDa or 75-kDa TNF receptors. *J. Biol. Chem*. **268**, 26350–26357.

35. Shingarova L.N., Sagaidak L.N., Turetskaya R.L., Nedospasov S.A., Esipov D.S., Korobko V.G. 1996. Mutant human TNF: Construction and some properties. *Bioorgan. Khim*. **22**, 243–251.

36. Reed C., Fu Z.Q., Wu J., Xue Y.N., Harrison R.W., Chen M.J., Weber I.T. 1997. Crystal structure of TNF-alpha mutant R31D with greater affinity for receptor R1 compared with R2. *Protein Eng*. **10**, 1101–1107.

37. Cha S.S., Kim J.S., Cho H.S., Shin N.K., Jeong W., Shin H.C., Kim Y.J., Hahn J.H., Oh B.H. 1998. High resolution crystal structure of a human tumor necrosis factor-alpha mutant with low systemic toxicity. *J. Biol. Chem*. **273**, 2153–2160.

38. Alejo A., Ruiz-Arguello M.B., Ho Y., Smith V.P., Saraiva M., Alcami A. 2006. A chemokine-binding domain in the tumor necrosis factor receptor from variola (smallpox) virus. *Proc. Natl. Acad. Sci. USA*. **103**, 5995–6000.

39. Bodmer J.L., Schneider P., Tschopp J. 2002. The molecular architecture of the TNF superfamily. *Trends Biochem. Sci*. **27**, 19–26.

40. Grell M., Wajant H., Zimmermann G., Scheurich P. 1998. The type 1 receptor (CD120a) is the high-affinity receptor for soluble tumor necrosis factor. *Proc. Natl. Acad. Sci. USA*. **95**, 570–575.

41. Gileva I.P., Nepomnyashchikh T.S., Antonets D.V., Lebedev L.R., Kochneva G.V., Grazhdantseva A.V., Shchelkunov S.N. 2006. Properties of the recombinant TNF-binding proteins from variola, monkeypox, and cowpox viruses are different. *Biochim. Biophys. Acta*. **1764**, 1710–1718.

42. DeLano W.L. 2002. *The PyMOL Molecular Graphics System*. Palo Alto, CA: DeLano Scientific. URL: http://www.pymol.org.